

On the Structural Differences Between Elevated and Flush-mounted Transverse Jets

P.R.E. Cutler and R.M. Kelso

Department of Mechanical Engineering
The University of Adelaide, South Australia, 5005 AUSTRALIA

Abstract

Flush-mounted and elevated jets in crossflow are studied using flow visualisation techniques. Significant differences are demonstrated which suggest that the presence of the flat wall of the flush-mounted jet leads to a significant increase in the mixing rate and a lower jet trajectory compared with the elevated jet. The reasons for these differences are discussed.

Introduction

The work presented in this paper is a result of a study being undertaken to investigate means of controlling the mixing of a transverse jet or jet in crossflow (JICF). As part of this work, comparisons were made between the mixing of a flush-mounted jet and that of an elevated jet. However, in the initial stages of this work, it emerged that the two flow cases are distinctly different. Although a small number of researchers have alluded to this difference, the authors of the current paper have not found any publications that directly compare the structure and mixing of the flows. The paper presented here discusses the differences in the flow structure between the two cases and suggests reasons for these differences.

Transverse jets occur both in nature and in many industrial processes. Natural examples include the smoke from a volcano or plumes from a fire, whereas industrial cases include the discharge of effluent into a waterway, or the smoke into the atmosphere from a stack. In most cases the ability to predict the mixing and therefore dispersion of the discharge is important, and further, means of increasing the rate of dispersion are beneficial. It is already understood that a transverse jet produces enhanced mixing compared with that of a free jet. This fact is generally attributed to the presence of counter-rotating vortices, which result from the interaction of the jet and the cross-flow. The question of how to maximise the mixing and dispersion of the jet fluid remains unanswered. Specifically, the effects of the jet and crossflow Reynolds number, jet-to-crossflow ratio and jet elevation are poorly understood.

The present study therefore sets out to investigate the near-field mixing of low Reynolds number circular jets discharging perpendicularly to a crossflow. Similar work has been undertaken before, in particularly that of Smith and Mungal [8] and Smith, Lozano, Mungal & Hanson [7]. That research was undertaken on jets with high velocity ratios and Reynolds numbers and dealt with the far field mixing. In addition, that work focused on the plane of symmetry between the vortices of the counter-rotating vortex pair (CVP). The contribution of this previous work to our understanding of the flow is significant, however, it is unclear whether centreplane measurements give a complete picture of the global development of the JICF structure. The present work sought to extend the previous studies by analysing scalar concentration data obtained on additional sectional planes, in particular to investigate the mixing along one of the counter-rotating vortices, and to consider the differences, if any, between a flush-mounted jet and an elevated jet.

Although the counter-rotating vortices are easy to identify by experimental techniques, predicting their location and trajectory for different flow cases is difficult due to the unsteady nature of the flow. It is therefore not possible to accurately align a laser sheet through the core of the vortices in order to gather the data necessary to generate the required concentration plots. Therefore, the concentration profiles were determined from data gathered on a series of planes within the flow. The data were then assembled and viewed using the volumetric visualisation software T3D, by Research Systems, Inc. When the data was displayed it became apparent that the structure of the flow for the flush-mounted jet and elevated jets are, in fact, quite different.

Although a difference in flow structure for flush and elevated jets had been discussed by Moussa *et al.* [6], who stated that the presence or absence of a rigid wall at the exit plane of the jet is crucial to the entire behaviour of the flow, particularly in the near field, their work largely focussed on the flush-mounted jet case. Eiff *et al.* [3], provided details of the interaction between the wake structures from the jet and chimney. The scalar field does not seem to have been investigated for the elevated flow case, nor is a direct comparison made between the flush and elevated flow cases.

Experimental Arrangement

Apparatus

The experiments were conducted in the 0.5 m x 0.5 m water channel situated in the Department of Mechanical Engineering at Adelaide University. A schematic diagram of the jet apparatus used is shown in Figure 1 with the coordinate system defined. Two configurations, an elevated jet and a flush-mounted jet at a velocity ratio of $R = 2$ were studied. Here the velocity ratio, R , is defined as the area-averaged velocity of the jet divided by the cross-flow velocity. The cross-flow velocity was 0.04 m/s for both cases, which yields a cross-flow Reynolds number of 2500, based on the cross-flow velocity and internal jet pipe diameter. A jet velocity of 0.08 m/s was used, hence the jet Reynolds numbers was 5000, based on the jet velocity and internal jet-pipe diameter.

The apparatus makes use of a false floor that can be placed in the working section of the channel to generate the flush-mounted jet or removed to provide the elevated jet case. This configuration allows the same jet pipe to be used for both cases, ensuring the same flow development length, approximately 5 jet diameters, from the contraction to the jet exit, for both cases. The circulation around the false floor is controlled via an adjustable rear spoiler. The jet exit velocity profiles, along the jet centreline plane ($z = 0$), were obtained for both flow cases using hydrogen bubble wire visualisation. A bubble wire was incorporated into the jet pipe approximately 3 jet diameters upstream of the jet exit.

Concentration data were obtained using planar laser induced fluorescence. Fluorescein dye at a concentration of 0.5 mg per litre of water was used as the jet fluid. A 5 Watt Argon-Ion laser was utilised, along with sheet forming optics mounted on a

traverse above the working section of the channel, to produce a 4 mm thick light sheet in the x-y plane which could be moved in the z-direction. Data were captured along 10 parallel planes, at 12 mm intervals, beginning at the jet centreline ($z = 0$ to $z = 108$ mm). At each plane 100 images were captured at a frame rate of 30 frames per second and with a 24 milli-second exposure using a Kodak MEGAPLUS ES1.0 10-bit camera. The images were stored as 16-bit TIFF images with no compression. Image analysis was undertaken using MATLAB.

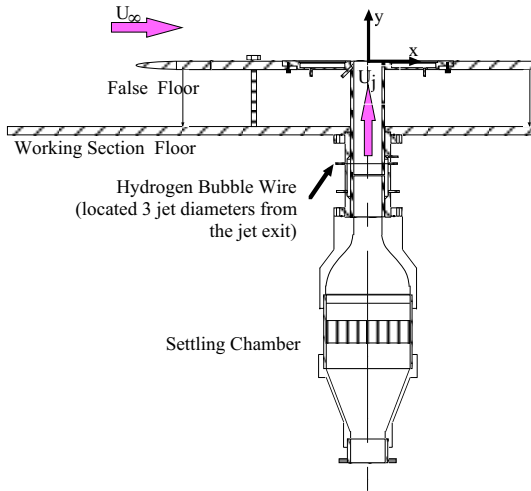


Figure 1. Schematic diagram of the jet apparatus used for the experiments. The false floor was removed to switch between the flush-mounted jet and elevated jet flow cases.

Data Processing: Image Concentration Correction

In order to extract the concentration data from the intensity images, corrections had to be made to calibrate the data. The correction scheme followed the format

$$C_{ij} = N \times \frac{(S_{ij} - SB_{ij})}{(L_{ij} - LB_{ij})} \quad (1)$$

where C_{ij} is ij th element of the corrected image, N is the factor to normalise the image by the 100% intensity level, S_{ij} is the image captured during the ij th element experiment, SB_{ij} is the ij th element of the averaged background image taken before each experimental run, L_{ij} is the corrected laser sheet profile and LB_{ij} is the averaged background laser profile image.

This scheme accounts for background intensity signal, which increases over the duration of the experiment due to the accumulation of dye in the water channel. It also accounts for any noise and the variation in the intensity of the laser beam due to the spreading of the laser beam to produce the sheet. It does not, however, take into account the absorption of the laser as it passes through the dyed region of the flow. The absorption was determined experimentally to be negligible.

Results

To visualise any differences between the concentration fields of the two flow cases, volumetric renderings of the averaged images were generated. By rendering only the portion of the flow at and above a particular concentration level, it is possible to determine where the jet fluid is most concentrated, corresponding to the trajectory of the counter-rotating vortices. Such renderings are shown in Figure 2. The images presented show the fluid with a concentration greater than 80% of the initial concentration of the jet fluid, rendered against the centreline and jet exit plane concentration slices.

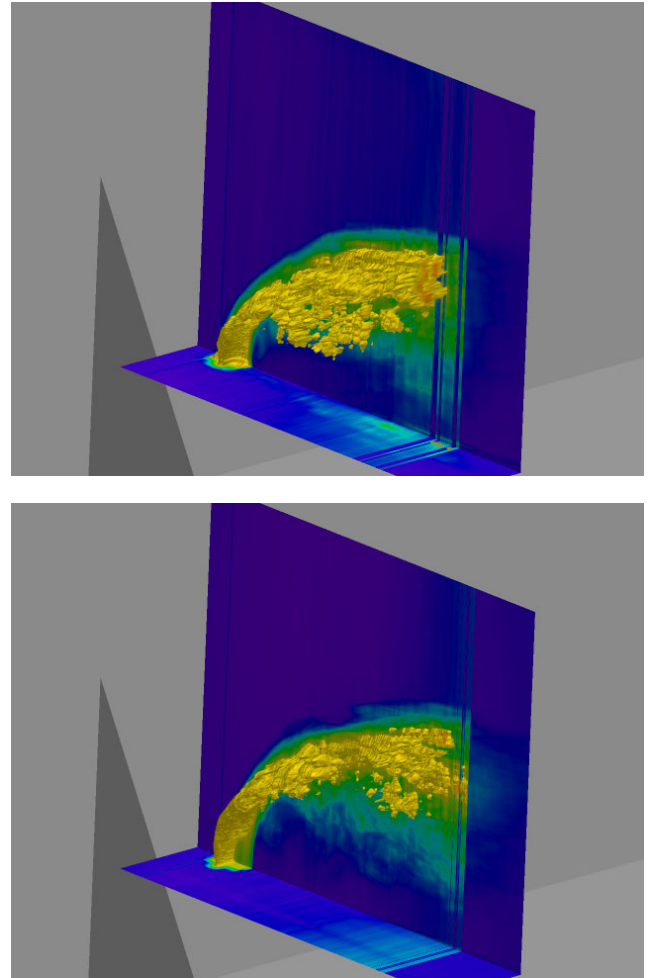


Figure 2. Volume rendering of the flow structures with a concentration level greater than 80% of the jet concentration, highlighting the trajectory of one of the counter-rotating vortices. The top image is for a flush-mounted jet and the bottom image for an elevated jet.

A number of important observations can be made from these results. First, the jet penetration is increased for the chimney flow compared with the flush-mounted jet. This is highlighted in Figure 3, in which instantaneous centreline images are presented for both flow cases. Second, within 2 jet diameters, the region of highest concentration occurs away from the jet centreline for the flush-mounted jet, but stays close to the centreline for the elevated jet. So the flush-mounted jet shows a lower trajectory and a more rapid lateral spreading.

In order to investigate the near field structure of the two flow cases, time lines for the two jet conditions were obtained by pulsing a bubble wire situated within the jet pipe, as shown in Figure 1. The resulting patterns are shown in Figure 4 and Figure 5 for the flush-mounted and elevated jet cases respectively. The time lines indicate the velocity profiles greater than one jet diameter upstream of the jet exit are similar to one another and symmetric about the jet centreline. Close to the jet exit the time lines remain similar to one another in terms of their slope and the indicated size of the separation within the pipe. Further from the jet exit, however, the time lines change substantially, particularly in the region of the upstream shear layer. In the case of the flush-mounted jet, the leading edge shear layer rolls-up in a periodic ring-like manner very close to the jet exit plane. By contrast the leading edge shear layer in the case of the elevated jet does not roll up until at least 2 jet diameters downstream of the jet exit.

To determine why this may be the case, a vertical hydrogen bubble wire was placed upstream of the leading edge of the false floor and positioned along the jet centreline. It was observed that, for the elevated case, a steady vortex is located on the leading edge, upper surface of the jet pipe. A close-up view of this vortex is shown in Figure 6. The vortex has a sense opposite to that of the jet shear layer, and probably forms due to the separation of the cross-flow fluid as it is drawn up the leading edge of the outer surface of the jet-pipe by the jet. The downstream trajectory of the core of this vortex is apparent from Figure 6. The angle of the core is consistent with a downwash in the wake of the elevated jet pipe. This is confirmed by additional observations. The down wash prevents substantial quantities of low momentum fluid behind the jet-pipe from being drawn into the jet.

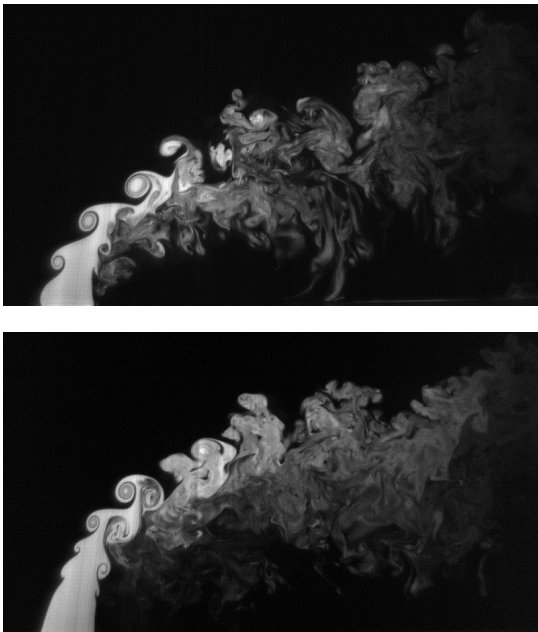


Figure 3. Instantaneous centreline PLIF images corrected for jet concentration. The upper image shows the case of a flush-mounted jet, whereas the lower image shows the elevated case.

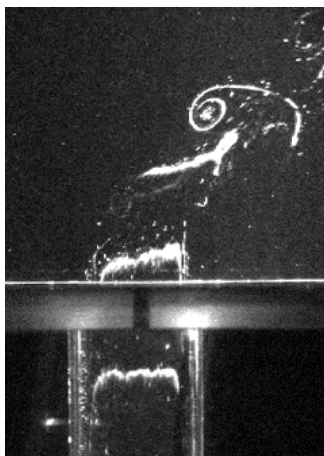


Figure 4. Time lines within the flush-mounted jet-pipe. The profiles were generated with a bubble wire positioned 3 jet diameters upstream from the jet exit.

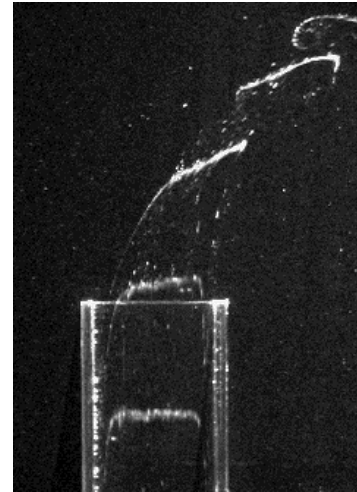


Figure 5. Time lines within the elevated jet-pipe. The profiles were generated with a bubble wire positioned 3 jet diameters upstream from the jet exit.

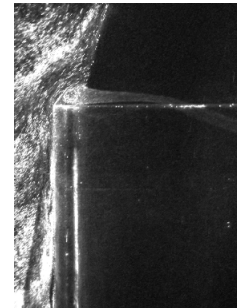


Figure 6. Close-up view of the leading edge of the jet-pipe focusing on the leading edge vortex. The image was produced using a hydrogen bubble wire upstream of the jet-pipe on the jet centreline.

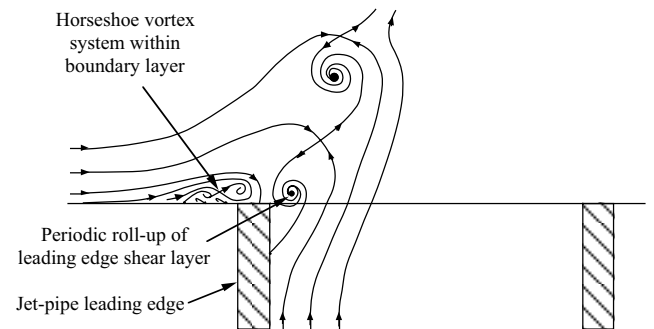


Figure 7. Interpretation of the flow structure for the flush-mounted jet case.

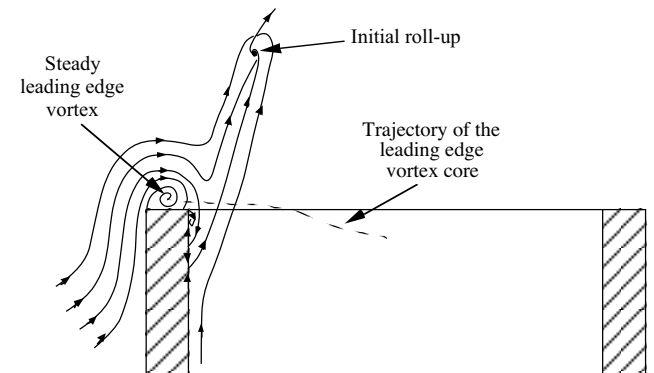


Figure 8. Interpretation of the flow structure shown in Figure 6 for the elevated jet.

Discussion

The two flow cases provide a means of investigating the effect of the wall and its associated boundary layer on the structure of a transverse jet. The major differences found between the two cases are the ring-like roll-up of the jet shear layer, the penetration of the jet into the cross-flow, the lateral spreading of the jet, and the trajectory of the high intensity jet fluid. It is believed these are all associated with different entrainment rates between the two cases. Although further work will have to be undertaken to establish the exact nature of the differences, some possible reasons are now presented.

Jet Shear Layer

The jet shear layer development appears to be quite different in the two cases, although the topological details are broadly similar. Interpretations of the flow patterns for the flush-mounted and elevated jet cases are presented in Figure 7 and Figure 8, respectively. The difference between the two flows comes about due to the difference in trajectory of the cross-flow fluid approaching the jet. For the elevated jet case, fluid approaching the upstream side of the jet is generally rising in the direction of the jet, as seen in Figure 6. This leads to the ring-like roll-up of the shear layer being delayed compared with the flush-mounted case. The elevated jet shear-layer appears to roll-up by a Kelvin-Helmholtz mechanism, beginning with a small instability near the jet exit and growing to large-scale eddies approximately 3 diameters from the exit. By contrast, the flush-mounted jet has a horizontal approaching stream and the shear layer in this case appears to roll-up within the pipe exit. The vortices that emerge are of a scale approaching a quarter of the pipe diameter. These processes are shown in Figure 6.

Jet Penetration and Mixing

A jet in cross-flow turns by the entrainment of fluid with horizontal momentum [1]. The greater the entrainment rate, the more rapidly the jet bends and the lower the overall trajectory. Therefore, we expect that any change in structure that increases entrainment will lead to a lower jet trajectory. One such change is the structure of the ring-like shear layer roll-up. The results demonstrate that when the shear-layer rolls up most rapidly, presumably leading to a greater entrainment rate, the jet bends more rapidly and the trajectory is lower.

A second aspect to this problem is the influence of the flat wall. One influence is to constrain the incoming flow so that it is normal to the jet at the jet exit. This leads directly to the differences in shear layer structures and entrainment as outlined above. Another influence of the flat wall comes to bear in the "wake" region of the jet. As shown by Fric and Roshko [5], the jet-crossflow interaction cannot generate vorticity away from solid boundaries and the crossflow cannot separate from the jet above the wall. However, Fric and Roshko did demonstrate that a momentum deficit exists in the near-wake region of a wall-mounted jet. Fric and Roshko identified that the deficit must be caused by low momentum wall boundary layer fluid and associated vorticity being lifted from the flat wall into the lee-side of the jet. This lifting process is governed by the CVP. This also provides a small pressure gradient across the jet that will increase the bending rate of the flush-mounted jet.

In the case of the elevated jet, flow visualisation studies show that there is a downwash in the wake near the top of the pipe. This prevents significant quantities of vorticity generated on the outer surface of the pipe from entering the wake of the jet and ensures that the fluid entrained into the wake originated mainly from the free stream. By the above arguments, the entrainment

of high-momentum (horizontal) cross-flow fluid into the lee-side of the jet would lead to a more rapid bending of the jet. Therefore, if entrainment by the CVP into the lee-side of the jet was the most significant contributor to the overall entrainment of the jet, then we would expect that the elevated jet would bend more rapidly than the flush-mounted jet. The observations presented in this paper show that the flush-mounted jet bends more rapidly than the elevated jet. This demonstrates that the ring-like roll-up of the shear layer on the upstream side of the jet has a larger influence on the overall entrainment than does the entrainment into the lee-side by the CVP. These conclusions apply to the near field of the jet.

The influence of entrainment on the circulation of the CVP is also of interest. Broadwell & Breidenthal [1] demonstrated that the circulation of the CVP is defined by the strength of the momentum source (the jet). This result is independent of the mixing rate. However, the present work has identified that there is an additional momentum source in the flush-mounted jet case, namely the flat wall. It is therefore likely that the circulation of the CVP in the flush-mounted jet will be different from that of the elevated jet. This concept may also explain the more rapid lateral spreading of the CVP in for the flush mounted jet identified in Figure 2. The difference in circulation may have an impact on the entrainment as discussed above.

Conclusions

The presence of the wall causes the jet shear layer to roll up more rapidly, closer to the jet exit. This increases the rate of entrainment of a flush-mounted jet compared with an elevated jet, and causes the flush-mounted jet to penetrate a shorter distance into the cross-flow. The results demonstrate that the ring-like roll-up of the shear layer provides the dominant entrainment mechanism in the near-field.

References

- [1] Broadwell, J.E. & Breidenthal, R.E. (1984) Structure and mixing of a transverse jet in incompressible flow, *Journal of Fluid Mechanics*, Vol. 148, pp. 405-412
- [2] Coelho, S.L.V., & Hunt, J.C.R. (1989) The dynamics of the near field of strong jets in crossflows, *Journal of Fluid Mechanics*, Vol. 200, pp. 95-120
- [3] Eiff, O.S. & Keiffer, J.F. (1997) On the structures in the near-wake region of an elevated jet in crossflow, *Journal of Fluid Mechanics*, Vol. 333, pp. 161-195
- [4] Fric, T.F. (1990) Structure in the Near Field of the Transverse Jet, Ph.D. Thesis, California Institute of Technology
- [5] Fric, T.F. & Roshko, A. (1994) Vortical structure in the wake of a transverse jet, *Journal of Fluid Mechanics*, Vol. 279, pp. 1-47
- [6] Moussa, Z.M., Trishka, J.W. & Eskinazi, S. (1977) The Near Field in the Mixing of a Round Jet with a Cross-stream, *Journal of Fluid Mechanics*, Vol. 80, Part 1, pp. 49 – 80
- [7] Smith S.H., Lozano, A., Mungal, M.G. & Hanson, R.K. (1994) Concentration Measurements in a Transverse Jet by Planar Laser-Induced Fluorescence of Acetone, *AIAA Journal* 23, (1), pp. 208-211
- [8] Smith, S.H. & Mungal, M.G. (1998) Mixing, Structure and Scaling of the Jet in Crossflow, *Journal of Fluid Mechanics*, Vol. 357, pp. 83-122
- [9] Smith, S.H. (1996) The Scalar Concentration Field of the Axisymmetric Jet in Crossflow, HTGL Report No. T-328, August 1996